Binary Hydrogen-Tetrahydrofuran Clathrate Hydrate Formation Kinetics and Models

Yorihiko Nagai, Hiroki Yoshioka, Masaki Ota, Yoshiyuki Sato, Hiroshi Inomata, Richard L. Smith, Jr.*
Tohoku University, Research Center of Supercritical Fluid Technology, Aoba-6-6-11, Aramaki Aza, Aoba-ku, Sendai 980-8579 Japan

Cor J. Peters
Faculty of Mechanical, Maritime and Materials Engineering, Dept. of Process and Energy, Delft University of Technology, Leeghwaterstraat 44, 2628 CA Delft, The Netherlands

DOI 10.1002/aic.11587
Published online September 24, 2008 in Wiley InterScience (www.interscience.wiley.com).

Binary H_2-THF clathrate hydrate formation kinetics were investigated with a pressure decay method at temperatures from 266.7 to 275.1 K, at initial pressures from 3.6 to 8.4 MPa, and at stoichiometric THF hydrate concentrations for particle sizes between 212 and 1,400 μm. Formation rate increased for smaller particle sizes, higher pressures and lower-temperatures. A hydrogen delocalization model and a proposed hydrogen hydrate phase diffusion (HHPD) model were used to analyze the formation mechanisms. The HHPD model assumes that the H_2-THF hydrate phase is formed due to hydrogen adsorption onto the particle surface that is followed by subsequent diffusion of hydrogen into the clathrate hydrate. The HHPD model could express the kinetics quantitatively at the experimental conditions studied. Values of the hydrogen diffusion coefficient in the clathrate hydrate estimated from the bulk data and the phase thickness in the HHPD model agreed well with the literature. © 2008 American Institute of Chemical Engineers *AIChE J,* 54: 3007–3016, 2008

Keywords: hydrogen storage, hydrogen hydrate, THF hydrate, formation rate, kinetic model

Introduction

Hydrogen clathrate hydrates have received considerable attention since their discovery in 1993 by Vos et al.[1] who found that hydrogen could occupy the voids of a crystalline water structure with a H_2:H_2O stoichiometry that was close to 1:1 at pressures greater than 2.3 GPa. Mao et al.[2] explored the topic in detail and synthesized a hydrogen clathrate hydrate with structure II (sII), in which two hydrogen molecules were confined into each of the 16 pentagonal dodecahedral (5^{12}) small (S-size) cages, and four hydrogen molecules were confined into each of the eight hexakaidodecahedron ($5^{12}6^4$) large (L-size) cages for a total of 64 hydrogen molecules for every 136 water molecules corresponding to a 5.0 wt % hydrogen molecule containing solid. Synthesis of the hydrogen clathrate hydrate required pressures on the order of 200 MPa and cooling to below 249 K, but once the hydrate was formed, it was stable at atmospheric pressure and at temperatures up to 145 K and even *in vacuo* (~10 kPa) at 78 K[2]. Lokshin and Zhao[3] presented a rapid method (<2 min) for the synthesis of hydrogen clathrate hydrate from ground ice-Ih and H_2 gas, but their method still required pressures from 50 to 200 MPa. Mao and Mao[4] realized that the topic was one of great technological importance for the hydrogen economy and synthesized other hydrogen-rich clathrate hydrates. Although many of the clathrate hydrates

Correspondence concerning this article should be addressed to R. Smith at smith@scf.che.tohoku.ac.jp.

proposed by Mao and Mao met or exceeded U. S. department of energy (DOE) target of 4.5 wt % by 2005,[4] their method required high-pressures in excess of 200 MPa for clathrate hydrate formation.

Udachin et al.[5] found a pressure dependence for the occupancy of H_2 in a double cubic structure II clathrates of tetrahydrofuran (THF) with H_2, with one mole of hydrogen occupying the S-cages in the structure at pressures up to 70 MPa and two moles of hydrogen being possible to occupy the S-cages at pressures above 70 MPa. However, much excitement was generated when Florusse et al.[6] discovered that the introduction of a guest molecule THF, which acted as a sII hydrate-forming promoter, led to a reduction of synthesis pressures of hydrogen clathrate hydrates by 60-fold, to pressures as low as 5 MPa. In that work, the authors concluded that a single H_2 molecule most likely occupied each of the S-cages. Further, the ^{1}H MAS NMR showed that TDF occupied most all of the L-cages and volumetric measurements performed by dissociation of the clathrate solids gave an average of approximately one H_2 molecule per S-cage. In another work, Lee et al.[7] showed that the amount of H_2 that is contained in sII clathrate hydrates could be tuned by varying the THF promoter concentration from stoichiometric (5.56 mol % THF) with all L-cages filled with THF, to much less than stoichiometric (0.15 mol % THF) with mostly unoccupied L-cages to give hydrogen-rich clathrate hydrates having hydrogen molecule content as high as 4.0 wt %. Strobel et al.[8] examined cage occupancy of hydrogen molecules with respect to THF promoter concentration, formation pressure, and time and demonstrated that only one hydrogen molecule occupies the S-cage at THF mole fractions from 0.5 to 5.56 mol % (stoichiometric), at pressures up to 60 MPa, and over formation periods of one week. Kim et al.[9] have proposed the existence of a critical guest concentration (CGC) that may help to understand the mechanism of occupancy. However, it would still seem that pressure, promoter concentration and possibly phase density play a role in the initial formation process of the hydrogen clathrate hydrate.Hydrogen clathrate hydrate has technological importance as a hydrogen storage material and this progress in this field has been highlighted in a article by Hu and Ruckenstein,[10] who note that some of the hurdles that remain to be tackled include synthesis methods, temperature constraints, and capacity. Some controversies in the literature will probably be resolved with further synthesis methods and phase equilibrium measurements. For the case of developing phenomenological models, however, both equilibrium data and kinetic data are needed, and are summarized next.

Three-phase coexistence data for the (H_2O + H_2 + THF) system were measured by Florusse et al.[6] over the temperature range from 279 to 296 K at pressures from 5 to 100 MPa. At lower pressures, from 0.1 to 13.3 MPa, and over the temperature range from 277.5 to 281.4 K, Hashimoto et al.[11] presented data for the 5.6 mol % THF hydrogen hydrate that agreed well with the higher-pressure data of Florusse et al.[6] Equilibrium data have also been reported for related systems by Hashimoto et al.[12] (H_2 + CO_2 + THF + H_2O) and by Zhang et al.[13] (H_2 + CH_4 + THF + H_2O). Measurements by Anderson et al.[14] show comprehensive equilibrium conditions over a range of THF concentration up to and over the stoichiometric limit of 5.6 mol % THF at temperatures from 260 to 290 K, and at pressures up to 45 MPa.

Models for describing the equilibrium occupancy of hydrogen in THF-water clathrate have been presented by Strobel et al.[8] who proposed a simple single adsorption Langmuir isotherm written in terms of the hydrogen fugacity and a single fitting constant for the S-cage. The model was able to correlate the low-pressure (<100 MPa) data to within experimental error at low-pressures (<70 MPa), and gave reasonable agreement both with the high-pressure results of Udachin et al.[5] and with the one hydrogen molecule per S-cage limit. Lee et al.[15] developed a procedure to calculate the equilibrium conditions for hydrogen containing clathrates, based on a generalization of the method of Lee and Holder[16,17] and the use of Langmuir constants. The model showed that hydrogen occupancy stabilized the structure and lowered equilibrium pressure as expected, however, the model assumed occupancies of 2 moles of hydrogen in the S-cage, and 4 moles of hydrogen in the L -cages, which is in conflict with recent data[8]. Kim et al.[9] have developed equilibrium models and proposed tuning mechanisms.

Formation and release kinetics of hydrogen clathrate hydrates were presented by Lee et al.[7] where it was shown that the less than stoichiometric promoter concentrations (0.2 mol %, 0.7 mol %) formed faster hydrogen clathrate hydrates than stoichiometric promoter concentrations (5.56 mol %), whereas dissociation rates were roughly similar for all hydrogen clathrate hydrates. No models or detailed interpretation were presented in that work.

Although there are some equilibrium data for hydrogen clathrate hydrates, insufficient data exist on hydrogen clathrate formation kinetics, and the data that are available are not well suited for model development. Specifically, in this study, we use conditions of single hydrogen molecule occupancies of S-cages in sII clathrate hydrate with stoichiometric amounts of THF to fully occupy the L-cages. We examine a hydrogen delocalization model,[18] in which the driving force is the difference of the gas and hydrogen hydrate fugacity as suggested by Englezos et al.[19] and a hydrogen hydrate phase diffusion model that is based on the models proposed by Bishnoi and Natarajan[20] and Kawamura et al.[18] and applied by Ota et al.[21] in studies on methane and CO_2 hydrates. Discussion of these models allows us to formulate plausible hydrogen hydrate formation mechanisms.

Experimental Methods

Materials

Distilled/de-ionized water having an electrical conductivity of 5.5 μS/m was used in the experiments. Hydrogen gas (99.99%, Iwaki Suiso) and tetrahydrofuran (99.5%, Wako Pure Chemical, Inc.) without stabilizer were used.

Apparatus

The experimental apparatus (Figure 1a) used for the hydrate formation and dissociation experiments consisted of a 129.8 cm^3 cell (Figure 1b) constructed of SUS 316 (AKIKO Co.), a feed system, a 302.6 cm^3 reservoir tank (Whitey, 304-HDF4-300), a cooling system and a laser Raman spectrometer (JASCO, NR-2000), with a holographic grating, CCD (Princeton Instruments, Inc.) detector, and a resolution of within $\pm$ 1 cm^{-1}. The formation cell was main-

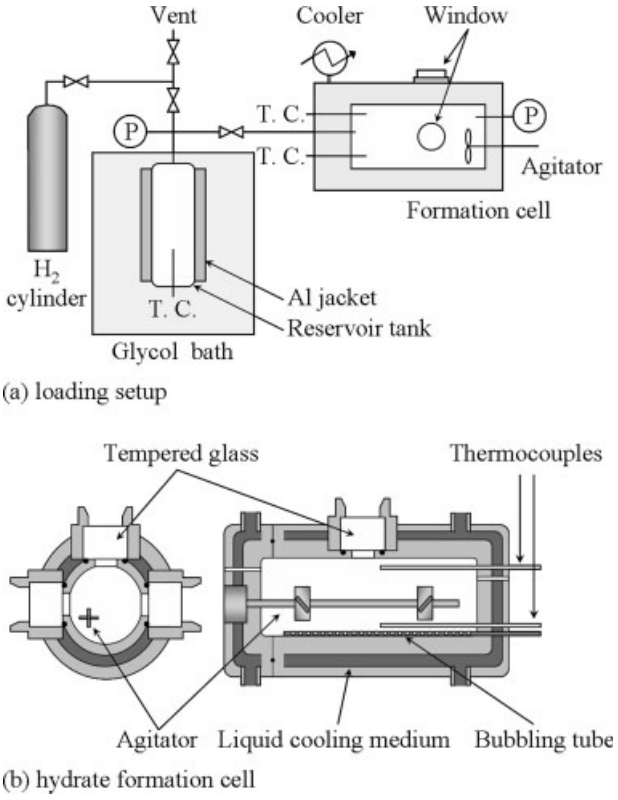

Figure 1. Schematic diagram of the apparatus for hydrate formation experiments: (a) loading setup, and (b) hydrate formation cell.

tained at the temperature of interest (266.7 to 275.1 K) to within ±0.2 K by an integral cooling jacket that was cooled by a circulator (LE-600, Advantec). The reservoir tank was maintained at the same temperature as that of the cell with a separate cooling unit (CA-1111, Eyela Co.). The cell (Figure 1b) had three windows with 90° spacing to allow for 180 and 90° Raman measurements. Two thermocouples were used to measure temperatures of the upper gas phase and the lower hydrate clathrate solutions. Temperatures in the cell and in the reservoir were measured with T-type thermocouples (CHINO) that were accurate to ±0.25 K. Pressures in the cell and reservoir were measured with independent pressure sensors (Setra, 280E) that were accurate to 0.11%, and which were confirmed with a secondary quartz pressure standard (DH-Budenberg, GPS II) to provide estimated maximum errors of 0.023 MPa. All temperatures and pressures were recorded by computer with a data logger (Agilent, 34970A).

Experimental procedure

Preparation of THF Hydrate. A THF solution of 5.56 mol % (19 wt %) was used to make about 60 g of THF hydrate. This solution was kept in a freezer at about 255 K for more than 1 day. The obtained THF hydrate was analyzed with Raman spectroscopy as shown in Figure 2a, which shows the obtained THF hydrate with liquid THF and THF solution. The THF hydrate was crushed with a mortar and pestle cooling under liquid nitrogen, and graded in a freezer according to particle size with SUS 316 sieves having sizes of 212, 355, 500, 600, 1,180, and 1,400 μm. The obtained THF hydrate particles were used immediately to avoid agglomeration and condensation.

Binary H_2-THF clathrate hydrate formation

After the cell and reservoir tank were cooled to the given temperature, about 10 g of THF hydrate particles were loaded. As soon as the system was evacuated by vacuum pump (Hitachi Koki Co., VR16L), the reservoir tank was pressurized to about 11 MPa with hydrogen gas and allowed to equilibrate. After temperature and pressure of the reservoir tank stabilized, which typically required a few minutes, the hydrogen gas was loaded into the cell over a period of about 10 min. From this time, pressure and temperature were recorded at 15 s intervals. The amount of hydrogen gas loaded $n_{H2,\ total}$, was calculated by the difference in hydrogen density before and after loading of the reservoir tank with the Soave and Redlich-Kwong (SRK) equation of state (EoS).[22] Density of the hydrogen gas in the cell was calculated at a given condition with the SRK EoS[22] at a given conditions. The amount of hydrogen in the hydrate phase

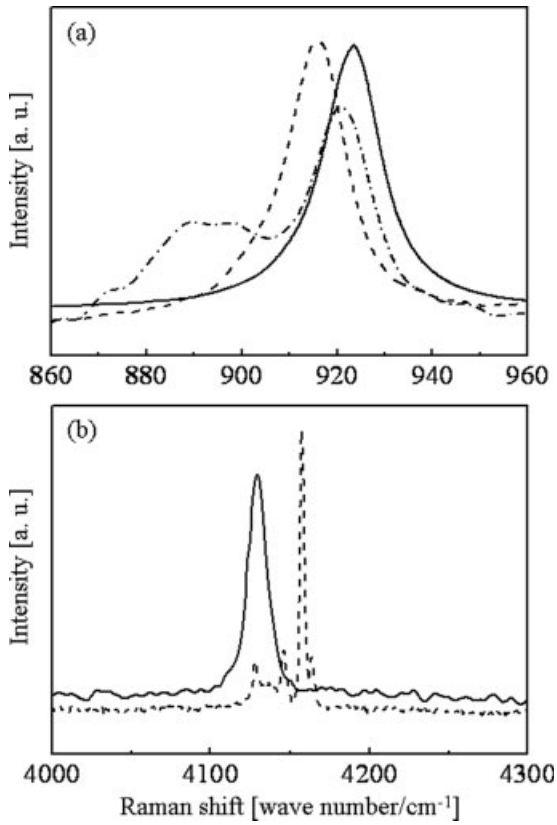

Figure 2. Raman spectra of obtained clathrate hydrates: (a) THF hydrate (solid line) with liquid THF (dashed line) and 19 wt % THF solution (dashed-dotted line) as reference, and (b) binary H_2-THF clathrate hydrate (solid line) with hydrogen gas (dashed line) as reference.

was calculated according to the pressure decay method[23–25] from the following relationships.

Water contained in hydrate phase

$$\rho_{H_2O,Hyd} = \frac{N^*_{H_2O} M_{H_2O}}{N_A a^3} \quad (1)$$

Volume of hydrate phase

$$V_{Hyd} = \frac{n_{H_2O} M_{H_2O}}{\rho_{H_2O,Hyd}} \quad (2)$$

Volume available to H_2 gas

$$V_{Gas} = V_{cell} - V_{Hyd} \quad (3)$$

Moles of free H_2 gas

$$n_{H_2,Gas} = \frac{\rho_{H_2,Gas} V_{Gas}}{M_{H_2}} \quad (4)$$

Moles of H_2 in hydrate phase by material balance

$$n_{H_2,Hyd} = n_{H_2,total} - n_{H_2,Gas} \quad (5)$$

where, $\rho_{H2O,\ Hyd}$ in Eq. 1 is the water density of that in the hydrate. As binary H_2-THF clathrate hydrate has sII structure, the lattice constant a was taken to be 17.3 Å and N^*_{H2O}, the theoretical number of water molecules per unit cell was taken to be 136. The volume of the hydrate phase V_{Hyd}, can be calculated from Eq. 2, which the volume occupied by the water molecules in clathrate hydrate form and the volume of the hydrate formation cell V_{cell} was taken to be as 129.8 cm^3. The amount of hydrogen in the gas phase, $n_{H2,\ Gas}$ was obtained by applying Eqs. 3 to 4. During hydrate formation, there is a vapor phase in the cell. In the calculations, it was assumed that the vapor pressures of H_2O and THF were negligible, which leads to the amount of hydrogen in the clathrate hydrate as shown by Eq. 5. The obtained binary H_2-THF clathrate hydrate was analyzed with *in situ* Raman spectroscopy as shown in Figure 2b to confirm hydrogen clathrate formation.

Results and Discussion

Table 1 summarizes the experimental runs made and their conditions. Experiments were made for various particle sizes from 212 to 1,400 μm, at initial pressures from 3.6 to 8.4 MPa, and at temperatures from 266.7 to 275.1 K. In this work, the uncertainty in the calculated number of moles of hydrogen in the hydrate was estimated to be to 3% based on pressure accuracy and the pressure decay region.

Table 1. Experimental Conditions for Hydrogen Hydrate Formation Experiments

Run	$W_{Hyd,\ 0}$ [g]	$W_{H2,\ 0}$ [g]	T [K]	Initial P [MPa]	d [μm]
1	8.98	0.720	269.5	6.5	212 – 355
2	10.4	0.707	269.5	6.5	500 – 600
3	12.5	0.693	269.5	6.5	1180 – 1400
4	11.4	0.706	266.7	6.5	500 – 600
5	7.90	0.709	275.1	6.5	500 – 600
6	8.92	0.913	269.5	3.6	500 – 600
7	7.66	0.406	269.5	8.4	500 – 600

THF concentration for all runs was 19.1 wt %.

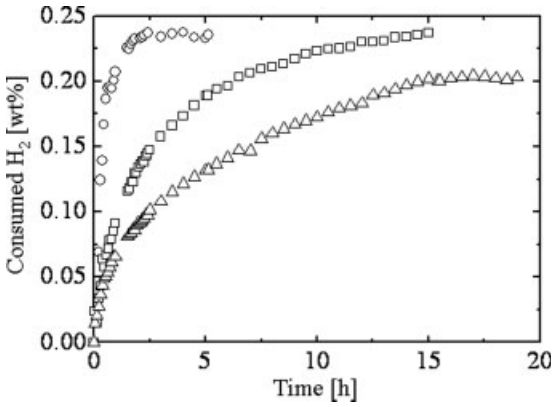

Figure 3. Hydrogen consumption as a function of time at 269.5 K, initial pressure of 6.5 MPa, and particle size of stoichiometric THF hydrate of 212 – 355 μm (circles), 500 – 600 μm (squares), and 1,180 – 1,400 μm (triangles).

Formation kinetics for various particle sizes

Figure 3 shows hydrogen consumption as a function of time for various particle sizes of stoichiometric THF hydrate clathrate at 269.5 K and initial pressure of 6.5 MPa. Hydrogen consumption is expressed as the ratio of hydrogen in hydrate phase to loaded THF hydrate by mass. The hydrogen consumption rate increased with decreasing particle sizes and the fastest rate was observed for particle sizes in the range of 212 to 355 μm. The differences in hydrogen uptake rates during 0 to 2 h are probably related to the surface areas of the different samples. The asymptotic values of particle sizes from 212 to 355 μm and from 500 to 600 μm seemed to approach the same value, however, the asymptotic value of 1,180 to 1,400 μm was noticeably lower than the values for the other particle sizes. For the 1,180 to 1,400 μm particles, although we followed the time evolution of hydrogen uptake until 19 h, the slow uptake would probably have to be continued for days or weeks or longer for to reach saturation. For the large particle sizes, it is possible that the hydrogen consumption rate was affected by both increases in the particle surface area, and the clathrate hydrate surfaces becoming saturated with hydrogen according to the available area. It would seem that hydrogen consumption depended on particle size and that diffusion of hydrogen was rate-controlled in the binary H_2-THF clathrate hydrate formation process.

Formation kinetics for various pressures

Figure 4 shows the rate of binary H_2-THF clathrate hydrate formation at 269.5 K, and various initial pressures beginning from stoichiometric THF hydrate having particle sizes between 500 and 600 μm. The initial hydrogen uptake rates were similar for the various pressures studied. The trends are an indication that free surface area was dominant in the initial adsorption process. On the other hand, initial stages are significantly influenced by heat transfer during

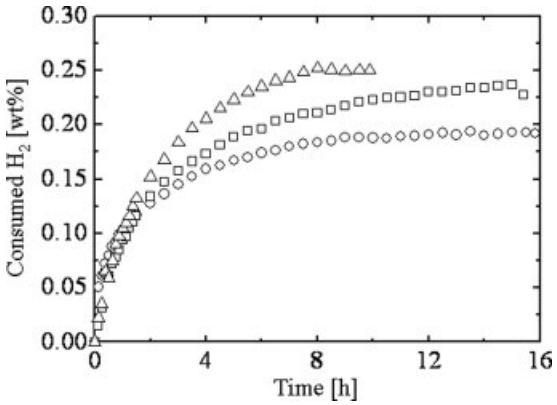

Figure 4. Hydrogen consumption as a function of time at 269.5 K, particle size of stoichiometric THF hydrate of 500 – 600 μm, and initial pressure of 3.6 MPa (circles), 6.5 MPa (squares) and 8.4 MPa (triangles).

The quasi-equilibrium occupancy of hydrogen in S-cage, θ_{eq}, were 0.19, 0.24 and 0.25 at initial pressures of 3.6, 6.5 and 8.4 MPa, respectively.

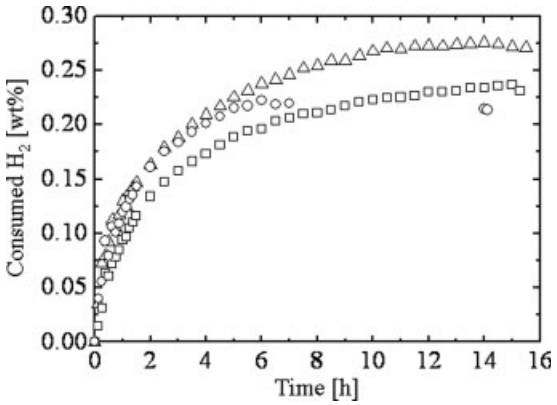

Figure 5. Hydrogen consumption as a function of time at initial pressure of 6.5 MPa, particle size of stoichiometric THF hydrate clathrate of 500 – 600 μm and temperature of 275.1 K (circles), 269.5 K (squares) and 266.7 K (triangles).

The quasi-equilibrium occupancies of hydrogen in the S-cage, θ_{eq}, were 0.24, 0.22 and 0.21, at 266.7, 269.5 and 275.1 K, respectively.

pressurization including heat of adsorption at the interface, so that estimation is difficult. The asymptotic values of the curves increased with increasing initial pressure. This binary hydrate forms through Langmuir type adsorption processes like the other common hydrates, so that the trend of hydrogen consumption at saturation conditions where hydrogen adsorption accelerates when pressure increased is the same trend as that reported by Strobel et al.[8] The total hydrogen consumption rate increased with increasing pressure, which means that diffusion of hydrogen into the hydrate phase also probably increased with pressure. On the other hand, the diffusion coefficient in the hydrate phase decreases with increasing pressure as reported by Okuchi et al.[26] who measured the diffusion of hydrogen into solid THF hydrate particle using pulsed field gradient NMR directly.

Formation kinetics for various temperatures

Figure 5 shows the rate of binary H_2-THF clathrate hydrate formation at 6.5 MPa, and temperatures ranging from 266.7 to 275.1 K beginning from stoichiometric THF hydrate having particle sizes between 500 and 600 μm. When temperature increased from 266.7 K to 269.5 K, hydrogen consumption decreased. This trend with temperature was the same as that expected for physical adsorption, which is an exothermic process. However, the variation of consumption rate with temperature can be expected to dependent on several factors, and so this topic will be discussed in a later section after introduction of the models.

Hydrogen occupancy

The data in Figures 4 and 5 appeared to reach steady-state values, which was taken as the quasi-equilibrium occupancy of hydrogen in the S-cages of binary clathrate hydrate. The hydrogen occupancy in S-cage θ_S, was taken to be the global occupancy and expressed as the ratio of number of entrapped S-cages to all S-cages expressed by Eq. 6

$$\theta_S = \frac{N^*_{H_2O}}{N^*_{H_2}} \frac{W_{H_2}}{M_{H_2}} \frac{M_{H_2O}}{W_{H_2O}} \tag{6}$$

where, N^* is theoretical number of molecules per unit cell so that for H_2O this value is 136, and for H_2 this value is 16 assuming single occupancy, which follows from the reports by Strobel et al.[8] and Anderson et al.[14] and the low-pressure ranges used in this work.

Figure 6 shows hydrogen occupancies measured as a function of pressure along with the data of Strobel et al.[8] Those researchers measured the occupancy of hydrogen using a

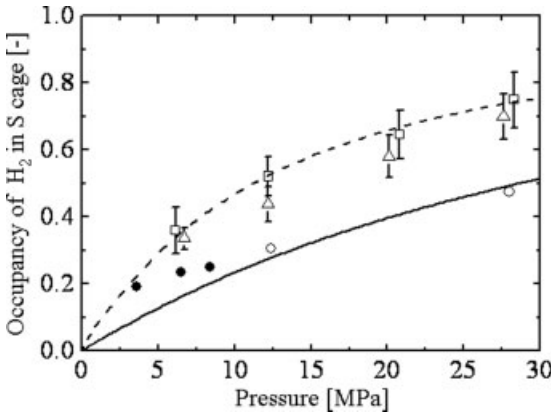

Figure 6. Hydrogen occupancies in the S-cages of stoichiometric H_2-THF binary hydrate as a function of initial pressure at 269.5 K and particle size of 500 – 600 μm in this work (filled circles).

Data of Strobel et al.[8] ^{1}H NMR method (circles), pressure decay method using particle size of 45 μm (squares) and 250 μm (triangles). Best fit Langmuir isotherm thorough ^{1}H NMR data, C_{H2} = 0.029 MPa^{-1} (solid line), and 45 μm data, C_{H2} = 0.087 MPa^{-1} (dashed line).

pressure decay method and an NMR method. As shown in Figure 6, the hydrogen occupancies of this work were consistently lower than data from pressure decay method of Strobel et al.[8] but were closer to the results obtained by the NMR method. Figure 6 also shows a single Langmuir isotherm model fits to the data obtained from their pressure decay and NMR methods in the form Eq. 7

$$\theta_S = \frac{C_{H_2} f_{H_2}}{1 + C_{H_2} f_{H_2}} \tag{7}$$

In this model, hydrogen fugacity was calculated by SRK EoS,[22] and the Langmuir constant was calculated by Newton's method. The deviation between SRK EoS and Wagner EoS[27] for the hydrogen fugacity in measurement ranges of Strobel et al.[8] was 0.77% with the number of about 500 data. The Langmuir isotherm from NMR data of Strobel et al.[8] agreed well with our data. Although there are differences in experimental conditions such as formation time, temperature, particle size, or even detection method between this work and that of Strobel et al.[8] the hydrogen occupancy in the S-cage of binary H_2-THF clathrate hydrate was small (ca. 0.2%), at the pressures studied in this work.

Hydrogen delocalization model

Considering a binary H_2-THF clathrate hydrate formation model from THF hydrate, Kawamura et al.[18] constructed a hydrogen delocalization model in which hydrogen was rapidly delocalized into THF hydrate from the particle surface expressed by Eq. 8

$$\left(\frac{dn_{H_2}}{dt}\right)_P = kAn_{H_2O}\left(f_{Gas} - f_{eq}\right) \tag{8}$$

Figure 7 shows a conceptual diagram of this model. The driving force of gas consumption is the difference in fugacity of hydrogen between bulk and equilibrium conditions as has been suggested by Englezos et al.[19,24] for other hydrate systems, and who also proposed that the model include the process of gas absorption. In Eq. 8, k is a kinetic constant for binary clathrate hydrate formation, and A is the total surface area of the THF hydrate particles assuming a spherical geometry, which is calculated with an average value after sieving. In this analysis, it can be assumed that one THF molecule is entrapped in each L-cage, and only one hydrogen molecule at maximum is entrapped in each S-cage based on the finding of Strobel et al.[8] which is the basis for the hydrogen delocalization model used in this work. The equilibrium pressure at these temperature conditions can be considered to be almost

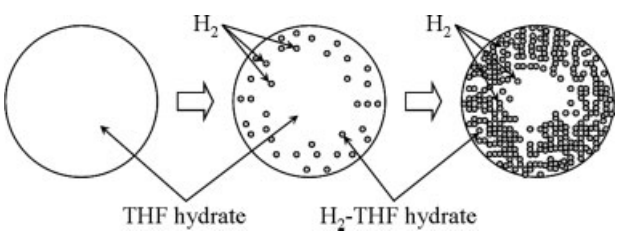

Figure 7. Conceptual diagram of hydrogen delocalization model based on reference.[18]

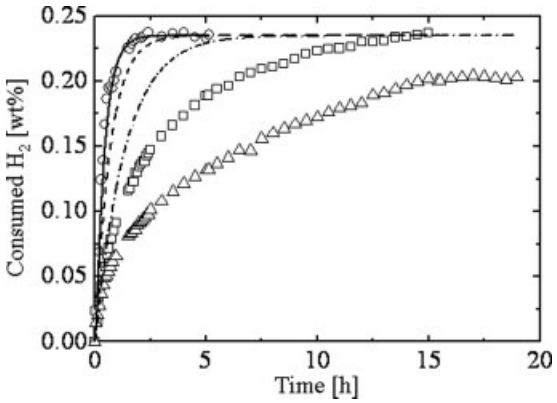

Figure 8. Estimation results of the hydrogen delocalization model for particle sizes of 212 - 355 μm (solid line), 500 – 600 μm (dash line) and 1,180 – 1,400 μm (dashed-dotted line).

Best fit hydrogen delocalization model parameter was $k = 3.5 \times 10^{-12}$ $(Pa{\cdot}s{\cdot}m^2)^{-1}$ that was determined from particle sizes of 212 – 355 μm. Symbols represents experimental values at 269.5 K, initial pressure of 6.5 MPa and particle size of stoichiometric THF hydrate of 212 – 355 μm (circles), 500 – 600 μm (squares) and 1,180 – 1,400 μm (triangles).

zero,[14] f_{eq} can be neglected. In this model, the surface area is considered to be constant, and the hydrogen consumption rate is proportional to the remaining amount of H_2O as shown by Eq. 9

$$n_{H_2O} = n_{H_2O,0}\left(1 - \frac{\theta_S}{\theta_{eq}}\right) \tag{9}$$

In Eq. 9, the θ_S used were the saturated adsorption values obtained from the quasi-equilibrium data in the experiments, which were comparable with the values reported by Strobel et al.[8]

The hydrogen delocalization model was evaluated with the assumptions mentioned previously. First, this model was correlated with the experimental data for particle sizes 212 – 355 μm, and the parameter k was determined. Then, the consumed hydrogen at other particle sizes was estimated using this value. Results are shown in Figure 8. Although the model could correlate the data for the small particle sizes, it could not express the particle size dependence as shown in Figure 8 for the case where the parameter k was used for the larger particle sizes. Therefore, it was apparent that there were other processes occurring that lead to a smooth reduction in the hydrogen consumption rate. In the next section, a model that considers hydrogen diffusion is developed.

Hydrogen hydrate phase diffusion (HHPD) model

The H_2-THF phase that is formed can be viewed as a result of hydrogen adsorption onto the particle surface, and then subsequent migration into the particle. For such migration, the hydrate formation rate should decrease gradually with the hydrogen consumption rate and depend on the diffusion of hydrogen into the phase. Figures 9 and 10 show a conceptual diagram of the model. In the clathrate hydrate formation process, two steps are considered. The first step is adsorption of hydrogen into the H_2-THF clathrate hydrate.

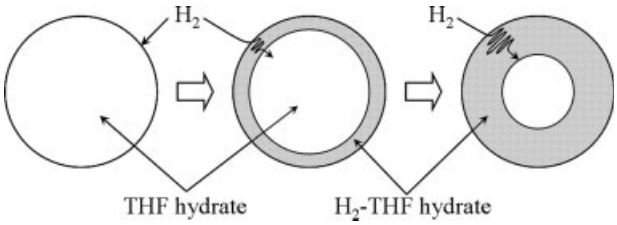

Figure 9. Conceptual diagram of hydrogen hydrate phase diffusion (HHPD) model.

The second step is diffusion of hydrogen into an empty S-cage. It is assumed that the following phases exist along with the reaction interface: THF hydrate phase, H_2-THF clathrate hydrate phase and a bulk gas phase. It is also assumed that all particles are spherical and single crystal, and in the binary clathrate hydrate, only one hydrogen molecule is entrapped in an S-cage under the experimental conditions. The assumption of up to a single hydrogen molecule in an S-cage at the given conditions is considered particularly valid in view of the recent measurements of Anderson et al.[14] who noted that only THF stabilizes the L-cage and according to their compositional analyses, that a 90% fill of S-cages by single hydrogen molecule (283 K, 30 MPa) occurs consistent with the data of Strobel et al.[8] The hydrogen hydrate phase diffusion (HHPD) model is expressed later.

The HHPD model incorporates a diffusion step, in which the driving force for hydrogen uptake is considered to be the difference between the hydrogen fugacity at the bulk and equilibrium conditions multiplied by an area and a mass-transfer coefficient k_d

$$\frac{dn_{H_2}}{dt} = k_d A \left(f_{Gas} - f_s\right) \tag{10}$$

The k_d was expressed as

$$k_d = \frac{D'_{H_2}}{L} \tag{11}$$

where L is the phase thickness of H_2-THF clathrate hydrate and D'_{H2} is an effective diffusion coefficient of hydrogen in the H_2-THF clathrate hydrate layer that contains mass-transfer contributions. It should be noted that D'_{H2} cannot be compared directly with hydrogen diffusion coefficients, since its units are those of mass transfer for the given phase thickness L. However, k_d should be directly proportion to the diffusion coefficient. The hydrogen hydrate phase thickness is given in terms of the instantaneous occupancy, θ_S/θ_{eq}

$$L = r - \left\{\frac{3V_{Hyd}}{4\pi N}\left(1 - \frac{\theta_S}{\theta_{eq}}\right)\right\}^{\frac{1}{3}} \tag{12}$$

as given in the Appendix. The adsorption step of hydrogen into the empty S-cage can be expressed by Eq. 13

$$\frac{dn_{H_2}}{dt} = k_a A \left(f_s - f_{eq}\right) \tag{13}$$

which is the same from as that used in the hydrogen delocalization model. At the initial stage of hydrate formation, A was calculated from the assumption of spherical particles as an average value after sieving, however, in this model, A was determined from Eq. 14 that assumes that A is proportional to the global occupancy

$$A = 4\pi N(r - L)^2 \tag{14}$$

In some sense, although the interfacial concentrations in this work are unknown, the phase thickness being variable, is consistent with the analysis of Sean et al.[28,29] who showed that the interface concentration of a dissociating hydrate particle is variable and depends on position of the spherical surface.

At equilibrium conditions or at the quasi-equilibrium conditions in this work, the lefthand side of Eq. 10 equals to that of Eq. 13. Then, Eq. 15 can be derived by eliminating f_s, which is the hydrogen hydrate fugacity at the interface as

$$\frac{dn_{H_2}}{dt} = 1 \Big/ \left(\frac{1}{k_a A} + \frac{L}{D'_{H_2} A}\right)\left(f_{Gas} - f_{eq}\right) \tag{15}$$

The HHPD model was evaluated in a similar way as that used for the hydrate delocalization model. Namely, the small particle size data were fit and then the results were used to study the particle size trends. Results are shown in Figure 11, where it can be seen that calculations agreed fairly well with the data. For calculation of A, although the particle size effect was compared based on the initial sieved values, the effect of particle size used as the initial value was relatively small, for k_a within $\pm 9\%$, and for D'_{H2} within $\pm 18\%$, so that it was used as the average particle radius for calculation. As shown in Figure 11, the model captured the trends of the formation rate, although for the 500 – 600 μm particle sizes, the model was systematically higher, which can probably be attributed to effect of initial heat transfer and possibly the competing factors of adsorption and diffusion. Since HHPD model was constructed under the assumption of two formation steps, adsorption and diffusion, in which the driving force is the difference between the hydrogen fugacity at the bulk and equilibrium conditions, the k_a and D'_{H2} should be

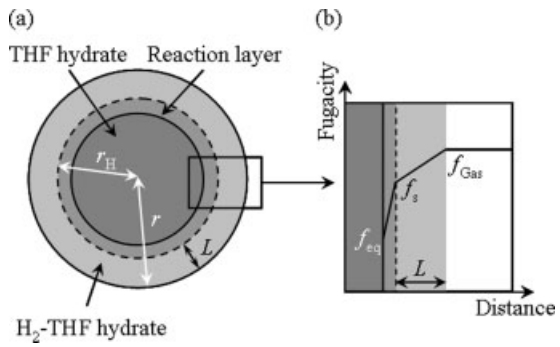

Figure 10. Conceptual diagram of hydrogen hydrate phase diffusion (HHPD) model: (a) phase assumption in the hydrogen hydrate phase diffusion (HHPD) model, and (b) fugacity driving force in the hydrogen hydrate phase diffusion (HHPD) model.

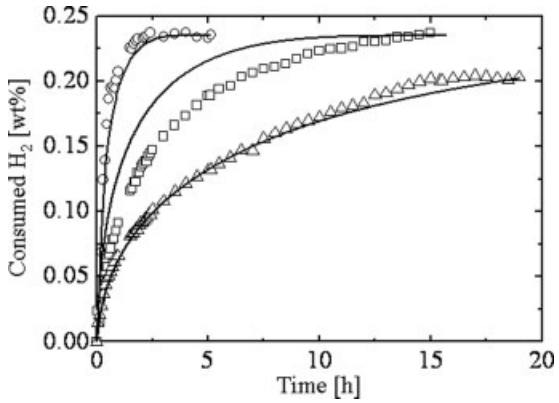

Figure 11. Estimation results of hydrogen hydrate phase diffusion model for particle dependence (solid line).

Best fit hydrogen hydrate phase diffusion model parameter were $k_a = 1.2 \times 10^{-11}$ mol/(Pa·s·m^2), and $D'_{H2} = 1.3 \times 10^{-16}$ mol/(Pa·s·m), that were determined from particle sizes of 212 – 355 μm. Symbols represents experimental values at 269.5 K, initial pressure of 6.5 MPa and particle size of stoichiometric THF hydrate of 212 – 355 μm (circles), 500 – 600 μm (squares) and 1,180 – 1,400 μm (triangles).

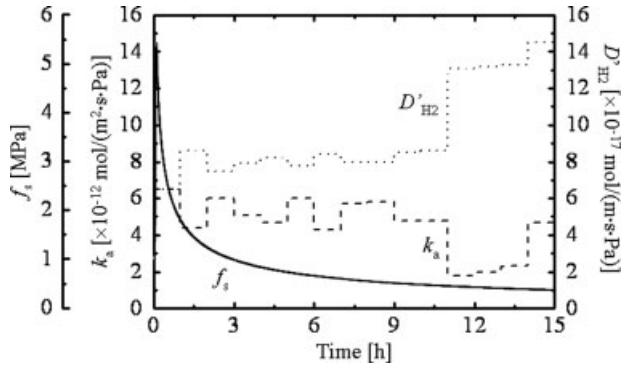

Figure 12. Time evolution of k_a (dash line) and D'_{H2} (dot line) values calculated for 1 h intervals for run 2, at 269.5 K, for an initial pressure of 6.5 MPa and particle sizes of 500 – 600 μm for stoichiometric THF hydrate.

Fugacity at the interface f_s (solid line), is shown as the hydrogen clathrate hydrate forms.

constant with time, at least, over some time-range. The time evolution of k_a and D'_{H2} were calculated at discrete intervals of an hour for one of the runs as shown in Figure 12. The values of k_a and D'_{H2} were relatively constant until 11 h from start of measurement indicating steady inclusion of H_2 into the clathrate hydrate structure. After 11 h, these values changed dramatically. This trend implies that there are two differential limiting stages in hydrogen clathrate hydrate formation, which includes an absorption controlled period before 11 h and a diffusion controlled period after 11 h. Time evolution of the hydrogen hydrate fugacity at the interface f_s, calculated with Eq. 10 is also as shown in Figure 12, and can be seen to steadily decrease. In Eq. 10, hydrogen uptake rate is proportional to surface area of binary H_2-THF clathrate hydrate A, which changes by formation period, and fugacity difference of between bulk gas phase f_{Gas} and f_s as driving force. Considering the over-all hydrate formation, f_{Gas} was almost constant as measured, although A decreased through binary hydrate formation according to the HHPD model. At quasi-equilibrium, f_s approached a value of about 0.5 MPa, which indicated hydrogen was not saturated in the S-cages.

Next, this model was applied to various conditions and the obtained parameters are shown in Table 2 and Figure 13 with the HHPD model. The HHPD model was fit to all of the runs using the absolute average deviation in moles as the objective function.

The trends of k_a and D'_{H2} with temperature, pressure, and initial surface area (particle diameter) of the hydrate particles are discussed next. In Table 2, for runs 2, 4 and 5, which have the same particles sizes and same initial pressure and different temperatures, the D'_{H2} was positively correlated with temperature, and this showed that hydrogen molecule diffusion kinetics in the binary H_2-THF hydrate layer was promoted by increasing temperature. For the k_a, there was little or no correlation with temperature. Comparing runs 2, 6 and 7 for the same particle sizes and same temperature at different pressures, the D'_{H2} and k_a varied only a slightly with pressure for the conditions in this study, which seems to support the use of the fugacity (pressure) driving force in the models. It should be also noted from Table 2 for runs of 1, 2 and 3 that the dependence of initial surface area (particle diameter) was relatively small, and this is supported in the discussion of Figure 11.

Diffusion coefficients D_{H2}, were estimated from the final slopes of the quasi-equilibrium data and the phase thickness of the model L, for each temperature. For the 500 to 600 μm particle sizes at an initial pressure of 6.5 MPa (runs 2, 4 and 5, Table 1), the estimated D_{H2} values were 3.6, 4.9 and 10.5 $\times 10^{-12}$ m^2/s, for 266.7, 269.5 and 275.1 K, respectively.

Activation energies of diffusion for hydrogen into the hydrate phase ΔE_D, and of adsorption ΔE_k, were calculated from the following relationships

Table 2. Fitted Parameters k_a and D'_{H2} for the Hydrogen Hydrate Pphase Diffusion Model

Run	Initial surface area [m^2]	k_a [mol/(Pa·s·m^2)]	D'_{H2} [mol/(Pa·s·m)]	Absolute Average deviation [mol]
1	2.0×10^{-1}	1.2×10^{-11}	1.3×10^{-16}	5.3×10^{-4}
2	1.2×10^{-1}	4.7×10^{-12}	8.2×10^{-17}	7.3×10^{-5}
3	6.0×10^{-2}	9.7×10^{-12}	1.6×10^{-16}	1.9×10^{-4}
4	1.3×10^{-1}	8.0×10^{-12}	1.1×10^{-16}	2.6×10^{-5}
5	8.9×10^{-2}	6.7×10^{-12}	1.8×10^{-16}	1.7×10^{-4}
6	8.6×10^{-2}	9.9×10^{-12}	1.6×10^{-16}	8.7×10^{-5}
7	1.0×10^{-1}	2.1×10^{-12}	1.7×10^{-16}	1.7×10^{-4}

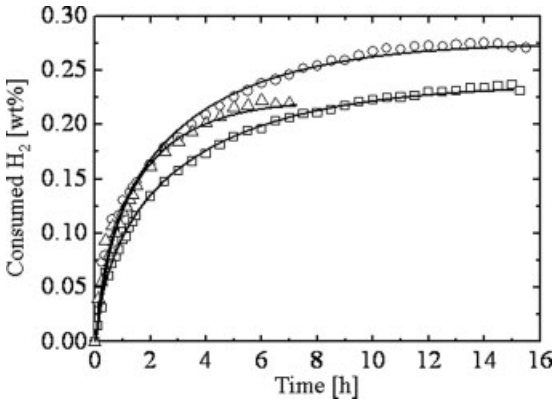

Figure 13. Correlation results of hydrogen hydrate phase diffusion model with temperature (solid line).

Best fit hydrogen hydrate phase diffusion model with data at temperatures of 266.7 K, $k_a = 8.0 \times 10-^{12}$ mol/(Pa·s·m^2) and $D'_{H2} = 1.1 \times 10^{-16}$ mol/(Pa·s·m), for 269.5 K, $k_a = 4.7 \times 10^{-12}$ mol/(Pa·s·m^2) and $D'_{H2} = 8.2 \times 10^{-17}$ mol/(Pa·s·m), and for 275.1 K, $k_a = 6.7 \times 10^{-12}$ mol/(Pa·s·m^2) and $D'_{H2} = 1.8 \times 10^{-16}$ mol/(Pa·s·m). Symbols represent experimental values at initial pressures of 6.5 MPa, particle sizes of stoichiometric THF hydrate of 500 – 600 μm and temperature of 266.7 K (circles), 269.5 K (squares) and 275.1 K (triangles).

$$D_{H_2} = D^*_{H_2} \exp\left(\frac{-\Delta E_D}{RT}\right) \tag{16}$$

$$k_a = k^*_a \exp\left(\frac{-\Delta E_k}{RT}\right) \tag{17}$$

From Eqs. 16 and 17, the obtained ΔE_D was 78.7 kJ/mol ($R^2 = 0.995$) and the ΔE_k was -5.9 kJ/mol ($R^2 = 0.02$). For the ΔE_k, the value agreed with intuition that the step of adsorption of hydrogen into an empty S-cage is exothermic, but this step did not show strong correlation with temperature over the ranges studied. The effect of the initial heat transfer was relatively large compared with the initial adsorption, which probably lead to the low correlation of k_a with temperature. Regarding the ΔE_D for gas molecules into the hydrate layer, Kuhs et al.[30] reported that the ΔE_D for methane was 52.1 kJ/mol through the neutron diffraction runs, and gas-consumption measurements from hydrogenated and deuterated ice powder. For carbon dioxide Genov et al.[31] reported that ΔE_D was 54.6 kJ/mol through the same method described previously, and for air, Salamatin et al.[32] reported ΔE_D was 50 kJ/mol although Raman spectra measurements of diffusive transport of the air constituents to hydrate crystal from air bubbles to polar ice sheets. The value of ΔE_D in this work (78.7 kJ/mol) was found to be somewhat higher than values for other gas molecules such as methane, carbon dioxide and air, that were in the range of 50 to 55 kJ/mol. In addition, Okuchi et al.[26] and Alavi and Ripmeester[33] have reported that ΔE_D for hydrogen molecule into the small cage were 3 $\pm$ 1 kJ/mol, and 23 – 28 kJ/mol, respectively. Frankcombe and Kroes[34] reported a ΔE_D of 32 $\pm$ 12 kJ/mol at high-pressure (150 MPa), and low-temperature (245 – 265 K) conditions, however, those simulations considered full occupation of hydrogens in the both S-cage and L-cage of the sII clathrate hydrate, which is not possible at the conditions used in this study. Although the ΔE_D values can greatly depend on the method or simulation assumptions, the value of ΔE_D estimated from the HHPD model in this work was found to be higher than those values, which may possibly be attributed to the bulk technique used in this work. On the other hand, the D_{H2} estimated in this study were on the order of 10^{-12} m^2/s, and these values were in close agreement with values reported by Okuchi et al.[26] at almost the same conditions. Okuchi et al.[26] reported that the diffusion coefficient of hydrogen in the binary H_2-THF clathrate hydrate was on the order of 10^{-12} m^2/s, and decreased with increasing pressure.

Conclusions

We investigated binary hydrogen-tetrahydrofuran clathrate hydrate formation kinetics. Hydrogen consumed rates and hydrogen occupancies in S-cages depended on temperature, initial pressure and particle size of the THF hydrates. When hydrate formation was assumed to consist of two steps, an adsorption step and a diffusion step, a model could be developed that could describe the experimental results both with respect to changes in particle size and variations with temperature or pressure. From this model, the activation energy of diffusion was estimated to be 78.7 kJ/mol, which was obtained from later portions of phase thickness change. To further explore the formation mechanism for increased hydrogen occupancies, we are considering the formation process from solution and in the presence of surfactants, which will be reported in a future work.

Acknowledgments

The authors wish to acknowledge support of Monbukagakusho, Ministry of Education, Culture, Sports, Science and Technology.

Notation

A = surface area of THF hydrate in hydrogen delocalization model; interfacial area between THF hydrate and H_2-THF hydrate in hydrogen hydrate phase diffusion model, m^2
A = lattice constant, m
C_{H_2} = Langmuir constant, Pa^{-1}
D_{H_2} = diffusion coefficient of hydrogen in binary clathrate hydrate phase, m^2/s
D'_{H_2} = effective diffusion coefficient of hydrogen in binary clathrate hydrate phase, mol/(Pa·s·m)
d = average particle diameter of hydrate, m
ΔE_k = activation energy of adsorption for gas molecule into the hydrate phase, J/mol
ΔE_D = activation energy of diffusion for gas molecule into the hydrate phase, J/mol
f = fugacity, Pa
f_{eq} = fugacity at equilibrium conditions (= 0), Pa
f_{Gas} = fugacity of gas phase, Pa
f_s = fugacity of interface between H_2-THF hydrate and reaction layer in hydrogen hydrate phase diffusion model, Pa
k = kinetic constant in hydrogen delocalization model, (Pa·s·m^2)$^{-1}$
k_a = kinetic constant of hydrogen adsorption in hydrogen hydrate phase diffusion model, mol/(Pa·s·m^2)
k_d = kinetic constant of diffusion in hydrogen hydrate phase diffusion model, mol/(Pa·s·m^2)
L = phase thickness of binary H_2-THF clathrate hydrate, m
M = molecular weight
N = particle number of hydrate
N_A = Avogadro's number
N^* = theoretical molecular number per unit cell

n = number of moles, mol
r = average particle radius of hydrate; distance between cage center and guest molecular, m
V = volume, m^3
W = loaded weight, g

Greek letters

θ_S = occupancy in S-cage
θ_{eq} = occupancy in S-cage under equilibrium conditions
ρ = density, kg/m^3

Subscripts

0 = initial conditions
cell = hydrate formation cell
Gas = gas phase
Hyd = hydrate phase

Literature Cited

1. Vos WL, Finger LW, Hemley RJ, Mao HK. Novel H_2-H_2O Clathrates at High-Pressures. *Phys Rev Lett*. 1993;71:3150–3153.
2. Mao WL, Mao HK, Goncharov AF, Struzhkin VV, Guo QZ, Hu JZ, Shu JF, Hemley RJ, Somayazulu M, Zhao YS. Hydrogen clusters in clathrate hydrate. *Science*. 2002;297:2247–2249.
3. Lokshin KA, Zhao YS. Fast synthesis method and phase diagram of hydrogen clathrate hydrate. *Appl Phys Lett*. 2006;88.
4. Mao WL, Mao HK. Hydrogen storage in molecular compounds. *Proc Nat Acad Sci USA*. 2004;101:708–710.
5. Udachin KA, Lipkowski J, Tkacz M. Double clathrate hydrates with helium and hydrogen. *Supramolec Chem*. 1994;3:181–183.
6. Florusse LJ, Peters CJ, Schoonman J, Hester KC, Koh CA, Dec SF, Marsh KN, Sloan ED. Stable low-pressure hydrogen clusters stored in a binary clathrate hydrate. *Science*. 2004;306:469–471.
7. Lee H, Lee JW, Kim DY, Park J, Seo YT, Zeng H, Moudrakovski IL, Ratcliffe CI, Ripmeester JA. Tuning clathrate hydrates for hydrogen storage. *Nature*. 2005;434:743–746.
8. Strobel TA, Taylor CJ, Hester KC, Dec SF, Koh CA, Miller KT, Sloan ED. Molecular hydrogen storage in binary THF-H_2 clathrate hydrates. *J Phys Chem B*. 2006;110:17121–17125.
9. Kim DY, Park J, Lee JW, Ripmeester JA, Lee H. Critical guest concentration and complete tuning pattern appearing in the binary clathrate hydrates. *J Am Chem Soc*. 2006;128:15360–15361.
10. Hu YH, Ruckenstein E. Clathrate hydrogen hydrate - A promising material for hydrogen storage. *Angewandte Chem-Int Ed*. 2006;45:2011–2013.
11. Hashimoto S, Murayama S, Sugahara T, Sato H, Ohgaki K. Thermodynamic and Raman spectroscopic studies on H_2+tetrahydrofuran plus water and H_2+tetra-n-butyl ammonium bromide plus water mixtures containing gas hydrates. *Chem Eng Sci*. 2006;61:7884–7888.
12. Hashimoto S, Murayama S, Sugahara T, Ohgaki K. Phase equilibria for H_2 plus CO_2 plus tetrahydrofuran plus water mixtures containing gas hydrates. *J Chem Eng Data*. 2006;51:1884–1886.
13. Zhang Q, Chen GJ, Huang Q, Sun CY, Guo XQ, Ma QL. Hydrate formation conditions of a hydrogen plus methane gas mixture in tetrahydrofuran plus water. *J Chem Eng Data*. 2005;50:234–236.
14. Anderson R, Chapoy A, Tohidi B. Phase relations and binary clathrate hydrate formation in the system H_2-THF-H_2O. *Langmuir*. 2007;23:3440–3444.
15. Lee S, Yedlapalli P, Lee JW. Excess Gibbs potential model for multicomponent hydrogen clathrates. *J Phys Chem B*. 2006;110:26122–26128.
16. Lee SY, Holder GD. A generalized model for calculating equilibrium states of gas hydrates: Part II. *Gas Hydrates: Challenges for the Future*. 2000;912:614–622.
17. Lee SY, Holder GD. Model for gas hydrate epuilibria using a variable reference chemical potential: Part 1. *AIChE J*. 2002;48:161–167.
18. Kawamura T, Komai T, Yamamoto Y, Nagashima K, Ohga K, Higuchi K. Growth kinetics of CO_2 hydrate just below melting point of ice. *J Cryst Growth*. 2002;234:220–226.
19. Englezos P, Kalogerakis N, Dholabhai PD, Bishnoi PR. Kinetics of gas hydrate formation from mixtures of methane and ethane. *Chem Eng Sci*. 1987;42:2659–2666.
20. Bishnoi PR, Natarajan V. Formation and decomposition of gas hydrates. *Fluid Phase Equilib*. 1996;117:168–177.
21. Ota M, Morohashi K, Abe Y, Watanabe M, Smith RL, Inomata H. Replacement of CH_2 in the hydrate by use of liquid CO_2. *Ener Convers Manage*. 2005;46:1680–1691.
22. Soave G. Equilibrium constants from a modified Redlich-Kwong equation of state. *Chem Eng Sci*. 1972;27:1197–1203.
23. Malegaonkar MB, Dholabhai PD, Bishnoi PR. Kinetics of carbon dioxide and methane hydrate formation. *Can J Chem Eng*. 1997;75:1090–1099.
24. Englezos P, Kalogerakis N, Dholabhai PD, Bishnoi PR. Kinetics of formation of methane and ethane gas hydrates. *Chem Eng Sci*. 1987;42:2647–2658.
25. Vysniauskas A, Bishnoi PR. A Kinetic-Study of Methane Hydrate Formation. *Chem Eng Sci*. 1983;38:1061–1072.
26. Okuchi T, Moudrakovski IL, Ripmeester JA. Efficient storage of hydrogen fuel into leaky cages of clathrate hydrate. *Appl Phys Lett*. 2007;91:171903-1–171903-3.
27. Wagner W, Overhoff U. *Thermofluids*. Berlin: Spring-Veriag; 2005.
28. Sean WY, Sato T, Yamasaki A, Kiyono F. CFD and experimental study on methane hydrate dissociation Part I. Dissociation under water flow. *AIChE J*. 2007;53:262–274.
29. Sean WY, Sato T, Yamasaki A, Kiyono F. CFD and experimental study on methane hydrate dissociation. Part II. General cases. *AIChE J*. 2007;53:2148–2160.
30. Kuhs WF, Staykova DK, Salamatin AN. Formation of methane hydrate from polydisperse ice powders. *J Phys Chem B*. 2006;110:13283–13295.
31. Genov G, Kuhs WF, Staykova DK, Goreshnik E, Salamatin AN. Experimental studies on the formation of porous gas hydrates. *Am Mineralog*. 2004;89:1228–1239.
32. Salamatin AN, Lipenkov VY, Hondoh T, Ikeda T. Simulated features of the air-hydrate formation process in the Antarctic ice sheet at Vostok. *Annals Glaciology*. 1999;29:191–201.
33. Alavi S, Ripmeester JA. Hydrogen-gas migration through clathrate hydrate cages. *Angewandte Chem-Int Ed*. 2007;46:6102–6105.
34. Frankcombe TJ, Kroes GJ. Molecular dynamics simulations of Type-sII hydrogen clathrate hydrate close to equilibrium conditions. *J Phys Chem C*. 2007;111:13044–13052.

Appendix A

Evaluation of hydrate thickness L, with Eq. 12

A radius r_H, and a volume V_H, for each THF hydrate particle (see Figure 10) that hydrogen does not occupy can be written as follows

$$r_H = r - L \tag{A1}$$

$$V_H = \frac{4}{3}\pi r_H^3 \tag{A2}$$

where r is the average particle radius of the hydrate particle and L is the phase thickness of binary H_2-THF clathrate hydrate. Then, V_H can be written as a ratio $V_H/(V_{Hyd}/N)$, that is assumed to be proportional to the occupancy, θ_S, at any given time

$$V_H/\left(V_{Hyd}/N\right) = \left(1 - \theta_S/\theta_{eq}\right) \tag{A3}$$

where V_{Hyd} is the volume of all THF hydrate particles, and N is the number of THF hydrate particles. Eq. 12 results from combination of Eqs. A1 – A3.

Manuscript received Nov. 9, 2007, and revision received Jun. 13, 2008.